

Supporting Information

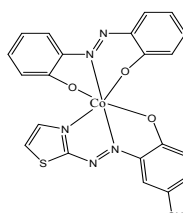
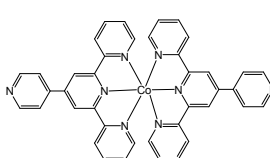
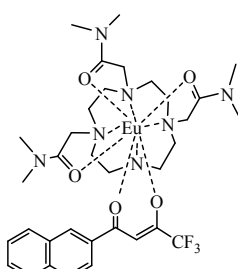
Cobalt metal-mixed organic complex-based hybrid micromaterials: ratiometric detection of cyanide

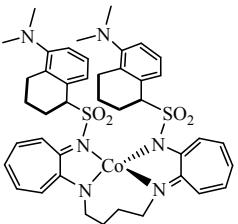
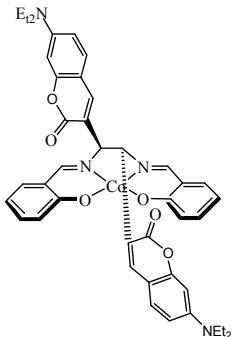
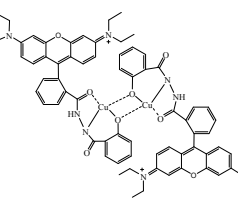
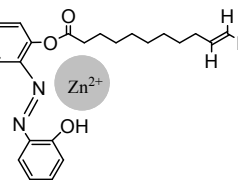
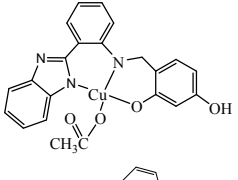
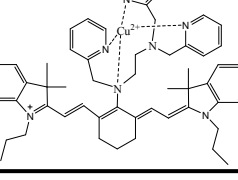
Hai-Bo Liu,* He-Song Han, Bin Lan, Dong-Mei Xiao, Jing Liang, Zi-Ying Zhang and
Jing Wang*

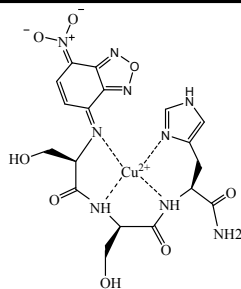
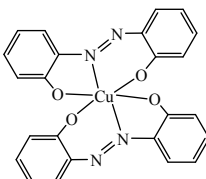
School of Chemistry and Chemical Engineering, Guangxi University, Nanning
530004, P. R. China

E-mail: lwllhb@gxu.edu.cn (H. B. Liu); wjwyj82@gxu.edu.cn (J. Wang)

Table S1 Comparison of a few recent examples for CN^- sensors based on organic-metal complexes

Complex	Mechanism	Specificity	Detection mode	Detection limit	pH	Ref.
	Strategy (iii)	CN^-	$A_{456\text{nm}}/A_{537\text{nm}}$	1.8 μM	2.5–9.5	This work
	Strategy (iii)	CN^-	$A_{450\text{nm}}, A_{517\text{nm}}$	10 μM	—	¹
	Strategy (iii)	HCO_3^-	$F_{616\text{nm}}$	—	7.5	²

	Strategy (iii)	NO	$F_{505\text{nm}}$	50-100 μM	—	2
	Strategy (ii)	CN ⁻ (no study for S ²⁻)	$F_{460\text{nm}}$	—	—	3
	Strategy (ii)	CN ⁻	$A_{562\text{nm}}, F_{580\text{nm}}$	0.14 μM	7.0	4
	Strategy (ii)	CN ⁻	$F_{550\text{nm}}$	30 nm	—	5
	Strategy (ii)	CN ⁻ (no study for S ²⁻)	$F_{600\text{nm}}, A_{495}/A_{325}$	—	5–11	6
	Strategy (i)	CN ⁻	$A_{400\text{nm}}$	4.0 μM	—	7
	Strategy (i)	CN ⁻ (no study for S ²⁻)	$F_{748\text{nm}}$	5 μM	2.7–10.4	4

	Strategy (i)	CN ⁻ (no study for S ²⁻)	A _{500nm} , F _{525nm}	724 nm	5.5–11.5	8
	Strategy (i)	CN ⁻ (no study for S ²⁻)	F _{590nm}	—	7.5	9

Abbreviations used: A—Absorbance; F—Fluorescence

Strategy (i): “displacement” approach;

Strategy (ii): “binding site—signaling subunit” protocol;

Strategy (iii): partial replacement of the bound ligand/antenna, accompanied by the formation of a new organic–metal–anion adduct;

References

- I. Bhowmick, D. J. Boston, R. F. Higgins, C. M. Klug, M. P. Shores, T. Gupta, *Sens. Actuators B*, 2016, **235**, 325–329.
- Z. Liu, W. He and Z. Guo, *Chem. Soc. Rev.*, 2013, **42**, 1568–1600.
- J. Wu, B. Kwon, W. Liu, E. V. Anslyn, P. Wang and J. S. Kim, *Chem. Rev.*, 2015, **115**, 7893–7943.
- F. Wang, L. Wang, X. Chen and J. Yoon, *Chem. Soc. Rev.*, 2014, **43**, 4312–4324.
- C. Parthiban, S. Ciattini, L. Chelazzi, K. P. Elango, *Sens. Actuators B*, 2016, **231**, 768–778.
- J. Wang and C.S. Ha, *Analyst*, 2011, **136**, 1627–1631.
- D. Wang, J. Q. Zheng, X. Yan, X. J. Zheng and L. P. Jin, *RSC Adv.*, 2015, **5**, 64756–64762
- K. H. Jung and K. H. Lee, *Anal. Chem.*, 2015, **87**, 9308–9314
- J. Wang and C.S. Ha, *Tetrahedron*, 2010, **66**, 1846–1851.

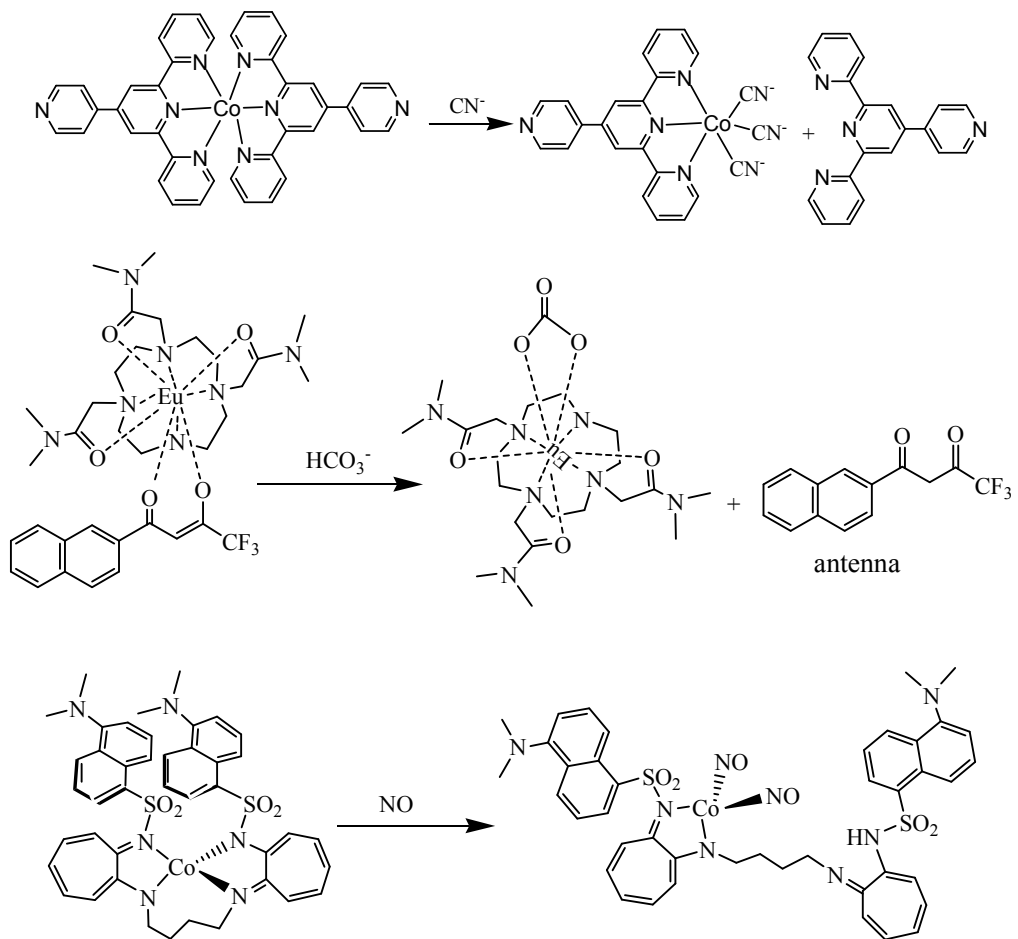


Fig. S1 Examples in Table S1 based on strategy (iii).

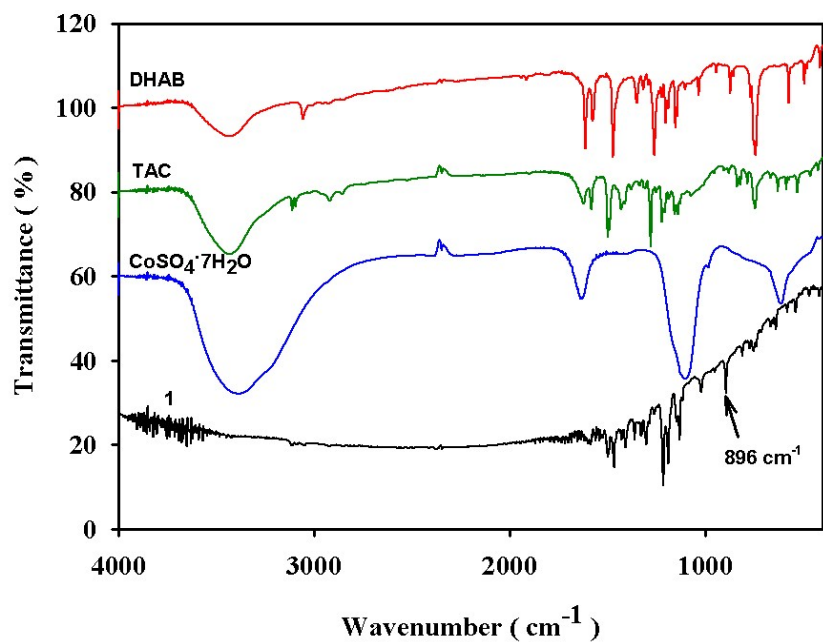


Fig. S2 FTIR spectra of DHAB, TAC, CoSO₄·7H₂O and complex **1**.

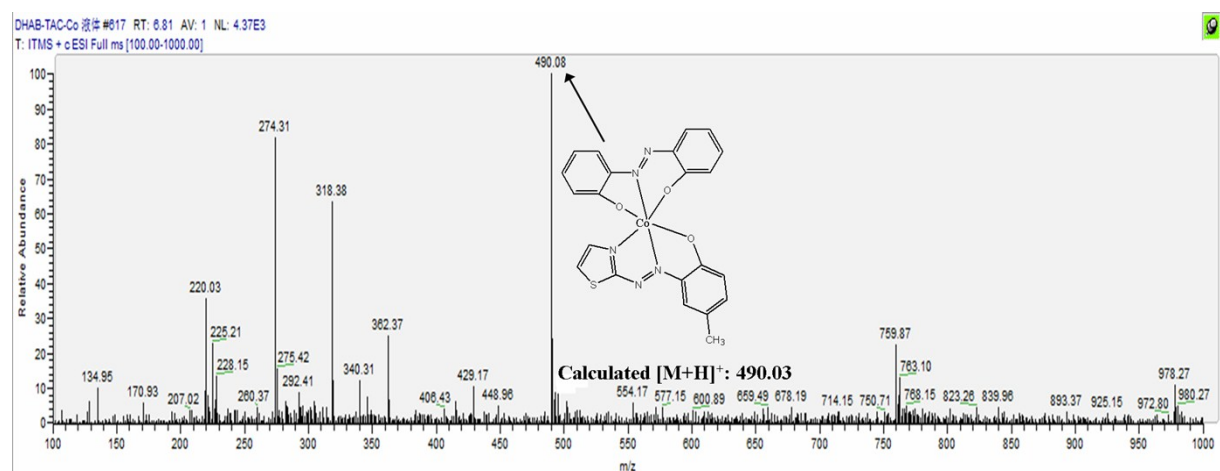


Fig. S3 QTOF-MS spectrum of **1** in acetonitrile.

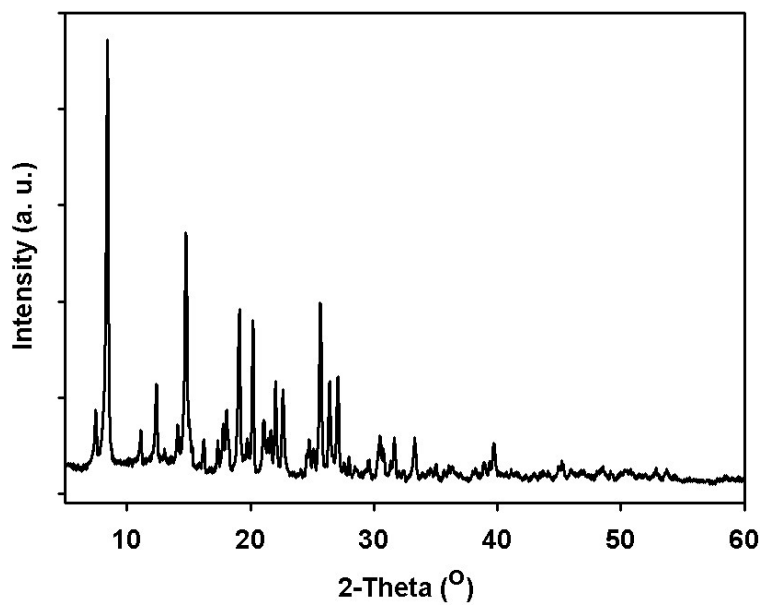


Fig. S4 Powder X-ray diffraction patterns of **1**.

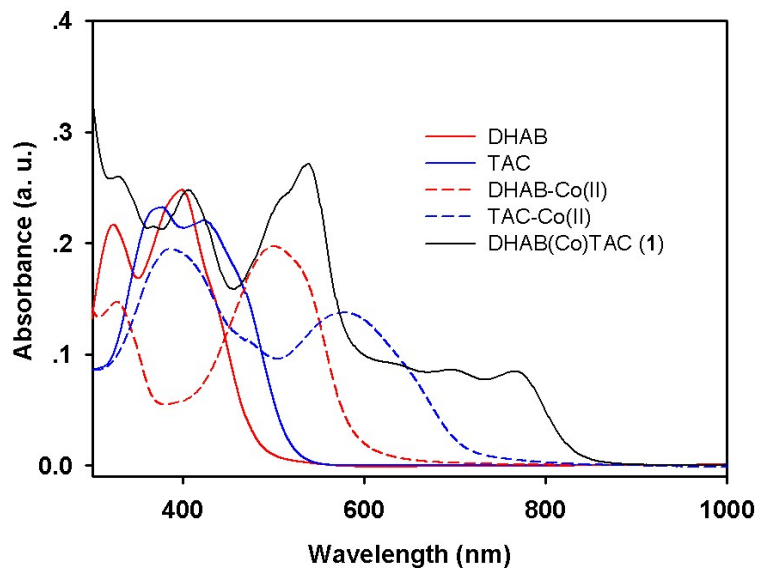


Fig. S5 Absorption spectra of DHAB (2×10^{-5} M) and TAC (2×10^{-5} M) in the absence and presence of Co^{2+} (1.0×10^{-4} M), and absorption spectra of complex **1** (2×10^{-5} M) in DMF-HEPES buffer solutions (4/1, v/v, pH 7.0).

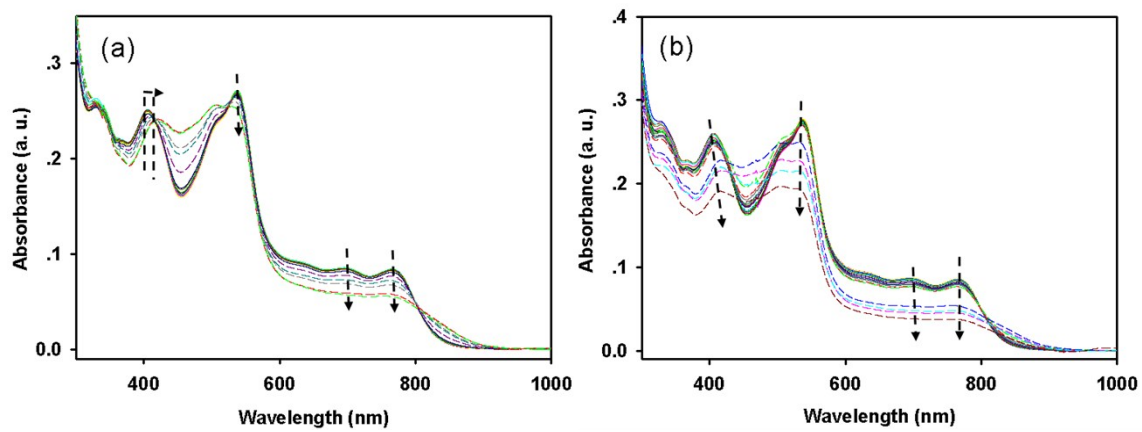


Fig. S6 Absorption spectra of **1** (2×10^{-5} M) upon titrating S^{2-} ($0\text{--}2.0 \times 10^{-3}$ M) (a) and SO_3^{2-} ($0\text{--}2.0 \times 10^{-3}$ M) (b) in DMF-HEPES buffer solutions (4/1, v/v, pH 7.0).

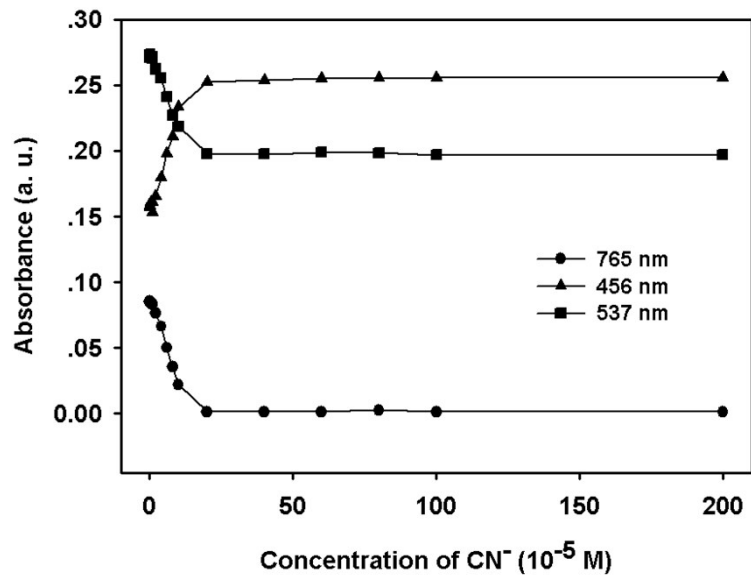


Fig. S7 Changes in the absorption spectra of **1** upon titrating CN^- ($0\text{--}2.0 \times 10^{-3}$ M) at 765 nm, 456 nm and 537 nm in DMF-HEPES buffer solutions (4/1, v/v, pH 7.0).

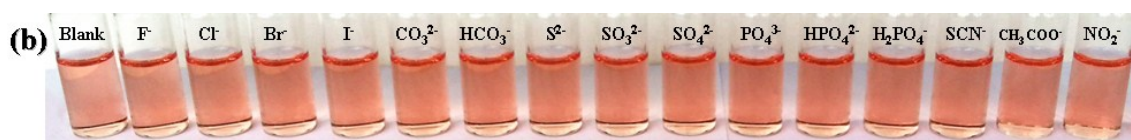
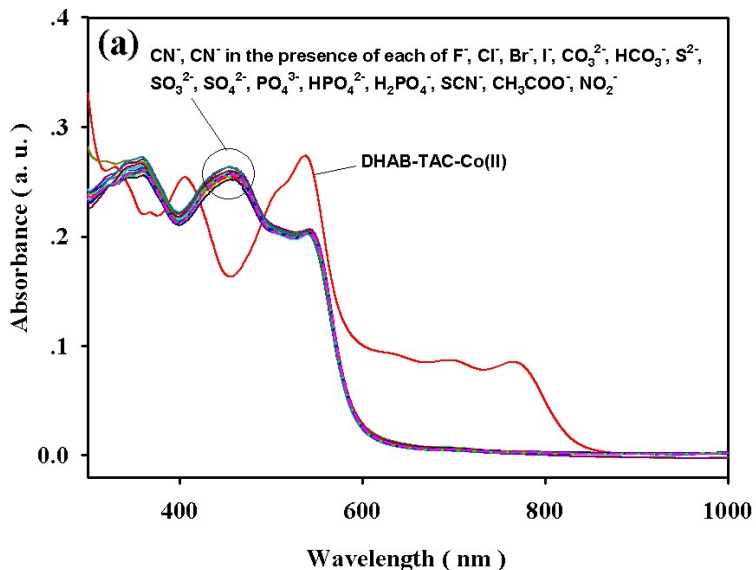


Fig. S8 (a) Absorption spectra and (b) visual colors of **1** (2×10^{-5} M) with 10 equivalents of CN^- and 20 fold concentrations of other anions with respect to CN^- , in DMF-HEPES buffer solutions (4/1, v/v, pH 7.0). Blank: **1** in the presence of 10 equivalents of CN^- .

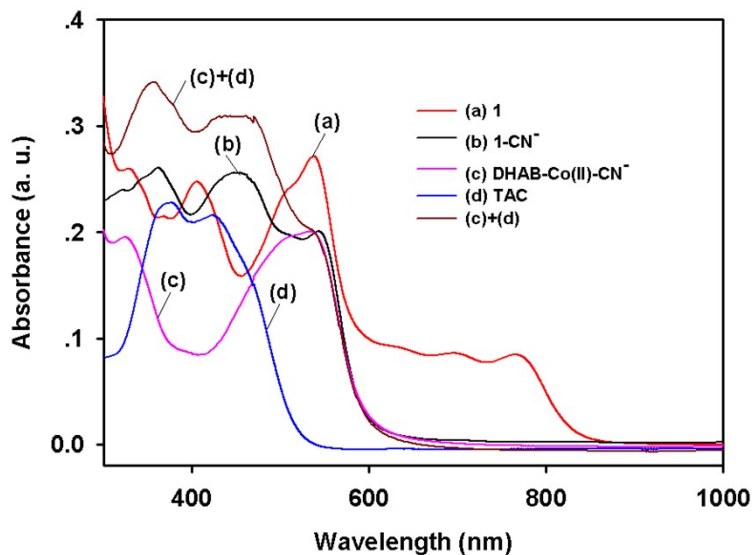


Fig. S9 Absorption spectra of **1** (2×10^{-5} M) in the absence (a) and presence of 10 equivalents of CN^- (b), and (c) absorption spectra of DHAB-Co(II) (2×10^{-5} M/ 2×10^{-5} M) in presence of 10 equivalents of CN^- , and (d) absorption spectra of TAC (2×10^{-5} M), in DMF-HEPES buffer solutions (4/1, v/v, pH 7.0).

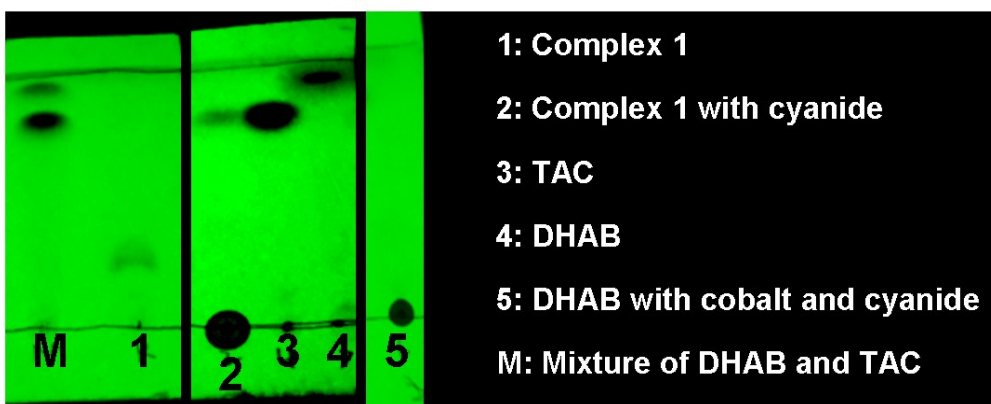


Fig. S10 TLC experiments of **1** with CN^- . The TLC plate was developed by 4:1 petroleum ether/ethyl acetate. Results indicated that TAC was released from complex **1** upon adding CN^- , while the dissociation of DHAB from complex **1** was not observed.

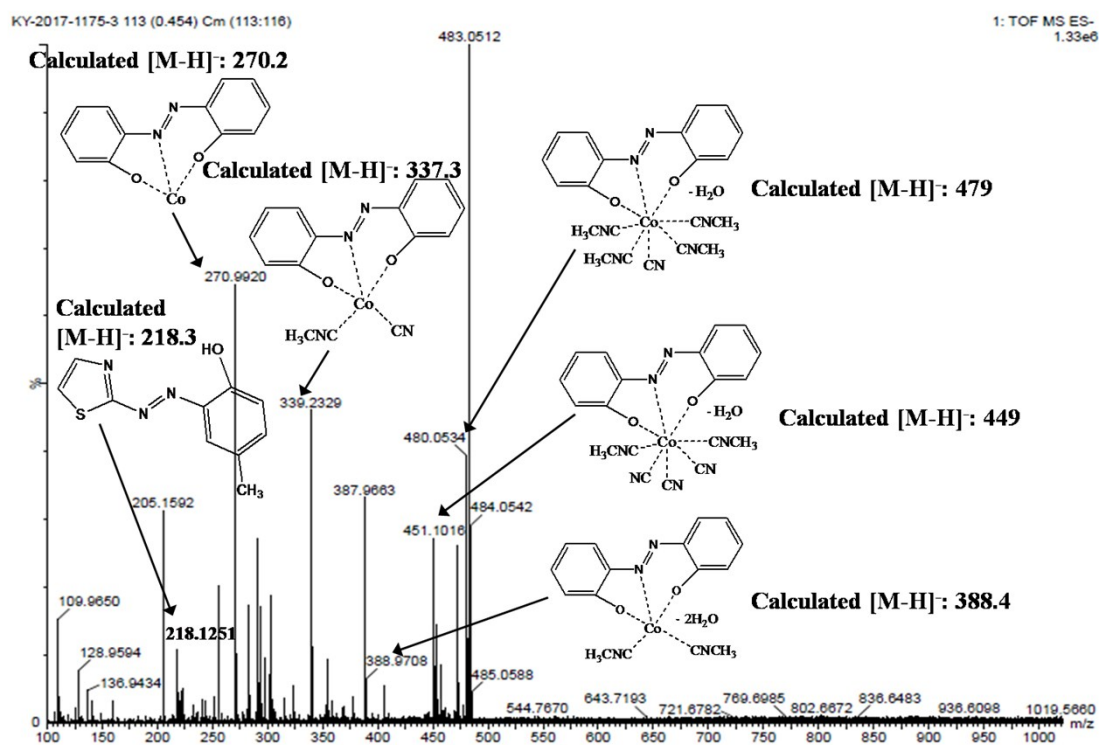


Fig. S11 QTOF-MS spectra of **1** with CN^- in acetonitrile.

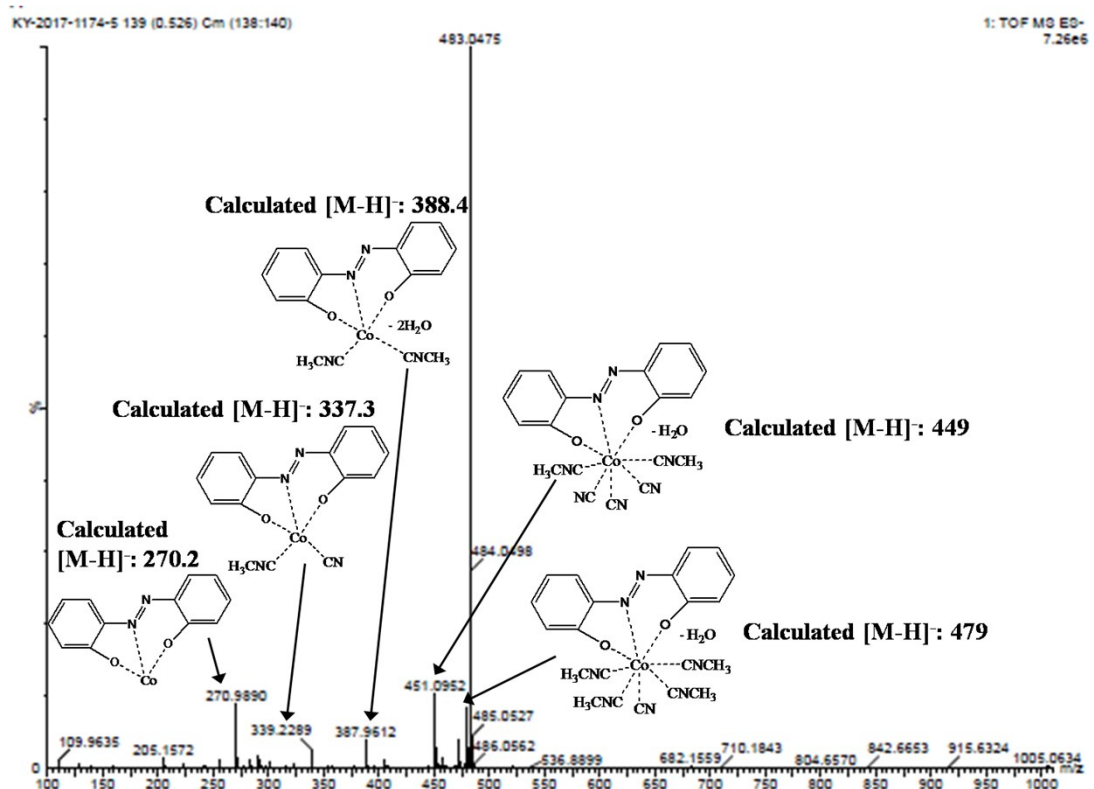


Fig. S12 QTOF–MS spectra of DHAB in the presence of Co^{2+} and CN^- in acetonitrile.

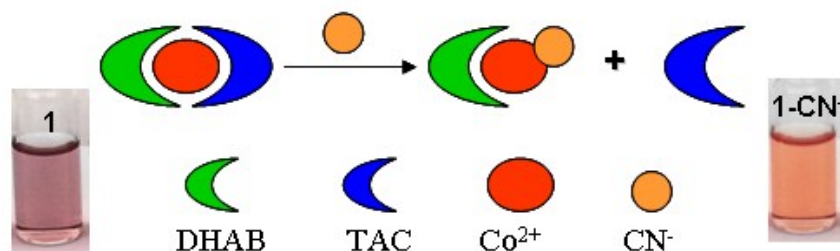


Fig. S13 Schematic illustration of CN^- detection using complex **1**.